

Assembly and Aerobic Photoreactivity of Melanin

John D. Simon, Yan Liu, and J. Brian Nofsinger
Department of Chemistry, Duke University
Department of Biochemistry, Duke University Medical Center

Introduction

Melanin refers to a group of biological pigments, which are commonly divided into two types: the black eumelanins, and the reddish-brown pheomelanins.¹⁻³ Eumelanins are composed of indolic units derived from the oxidation of tyrosine. Pheomelanins are composed of benzothiazine derivatives derived from the oxidation of cysteinyl-dopa molecules. Given that melanins are some of the most ubiquitous natural pigments, it may appear surprising their chemical structures and biological role(s) are still subject to debate. However, to date, it has proven impossible to assign a molecular structure to melanin.

Matrix-assisted laser desorption ionization time-of-flight mass spectrometry (MALDI-TOF MS), x-ray, neutron scattering techniques, and spatial imaging technologies provide important information about the molecular composition and structural morphology of melanins.⁴⁻¹² Synthetic eumelanins and eumelanin isolated from the ink sacs of the cuttlefish *Sepia officinalis* are the best-characterized systems. The melanin from *Sepia* is a pure eumelanin and can be isolated in quantities large enough to study using physical techniques. MALDI-TOF MS studies reveal molecular constituents in *Sepia* as well as other natural and synthetic eumelanin have molecular weights between 500 and 1500 amu.⁴ X-ray diffraction measurements of dried synthetic eumelanin have led to the proposal eumelanin is a highly crosslinked planar oligomeric structure containing ~4–5 indolequinone-like monomers.^{8,9} These oligomers are then believed to aggregate into a π -stacked structure containing 3–4 oligomers, often referred to in the literature as the fundamental aggregate. The pigment is hypothesized to be assembled from these π -stacked, crosslinked, and planar structures. Support for this model comes from images recorded using scanning tunneling microscopy (STM)¹⁰ and data on solutions of pure synthetic eumelanin and synthetic eumelanin in the presence of copper ions.⁷ On a larger distance scale, scanning electron microscopy (SEM) images of *Sepia* eumelanin suggest the pigment is an aggregated structure comprised of subunits having a lateral dimension on the order of 150 nm.¹³⁻¹⁵

Among various hypothesized functions, melanins are thought to be photoprotective, shielding the skin and eye against UV and visible (VIS) radiation.¹⁶ In the last few years we have carried out a variety of physical measurements aimed at furthering the understanding of the structure and photochemical properties of melanins. In the following sections we examine AFM studies on *Sepia* eumelanin and the role aggregation plays in affecting its aerobic photoreactivity.

Atomic Force Microscopy Studies of the Structure of Eumelanin

Figure 1A presents an SEM image of *Sepia* eumelanin granules. The typical granule measures tens of microns in diameter. Higher magnification reveals the surface is not smooth, Figure 1B. The granules share a common substructure; they appear to be comprised of closely packed spherical structures of diameters 150 ± 34 nm. This represents the natural structural morphology of the pigment.

Eumelanin is not very soluble in water, but material can be suspended and/or dissolved in water through sonication. Figure 2 shows an AFM image of material suspended in water through

Continued on page 3

From the Executive Director

D. C. Neckers, Executive Director, Center for Photochemical Sciences, Bowling Green State University

Something happened recently that caused me to look back at the textbook I used in organic chemistry as a student in the late 1950s. The organic chemistry I took predated Morrison and Boyd, so I'm embarrassed to even suggest whom the authors might have been. I remember we spent the first semester studying aliphatic compounds and the second semester studying aromatic compounds. The word *mechanism* may have shown up, but if it did I don't remember it. What struck me was how little in that well-worn textbook of another day I still use today. In another way, though, I was reminded of why chemistry intrigued me in the first place.

I remember that I liked my organic chemistry laboratory. It was a pretty dangerous place to be in those days. We ran Sandmeyer and Gattermann reactions, and I'm sure we crushed NaCN pellets under a non-working hood with a mortar and pestle. Washing our hands in organic solvents, benzene among them, was the best way to get rid of the grease. The sound of the fire extinguisher was very familiar. We often cut ourselves as we tried to force glass tubing through a cork stopper. We thought nothing about pouring bromine at our desktops from a flask. Cry we did, but when it happened we opened the windows. There were no instruments. Even melting points were taken in a bottle-like instrument filled with mineral oil and equipped with a thermometer. Breaking a mercury-filled thermometer was simply something to occupy our attention while an esterification reaction refluxed or an impure solid recrystallized. It was great fun to see the science labs janitor run from a pyridine soaked rag. An occasional pound of sodium filched from the stockroom to drop from a breakwall or sand dune into Lake Michigan could cause a heck of a racket.

Maybe I didn't become a chemist solely because of all the fun I had in my organic chemistry laboratory, but that fun sure didn't hurt. I was surprised when, as a TA in graduate school, I had to talk with my students about safety blankets, showers and kits. It was no wonder none of my students in those organic labs wanted to be chemists. Their laboratories were packaged and sterile. Most of the time they were able to get good yields, and if they didn't they didn't have to try the reaction until they did.

When I started this piece it was in the context of how little I do today relies on what I studied as an undergraduate. And that's still a true statement. But what I learned as an undergraduate is how much fun chemistry could be. I suppose, more than anything, my undergraduate experience prepared me for lifelong learning.

In This Issue

Assembly and Aerobic Photoreactivity of Melanin	1
From the Executive Director	2
Light-Based Detection Systems in Modern Gas Chromatography	7
Bistable Optoelectronic Device Realization by Photocurrent Bleaching	12
Center for Photochemical Sciences Publications	15

Continued from page 1

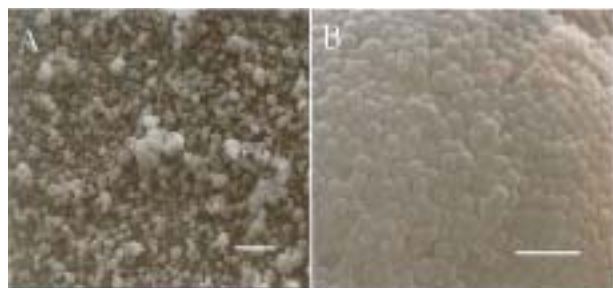


Figure 1. A. SEM image of melanin granules isolated from *Sepia* ink sacs. B. SEM image of the surface of a granule shown in (A). The white bars shown in images A and B correspond to distances of 500 μm and 500 nm, respectively.

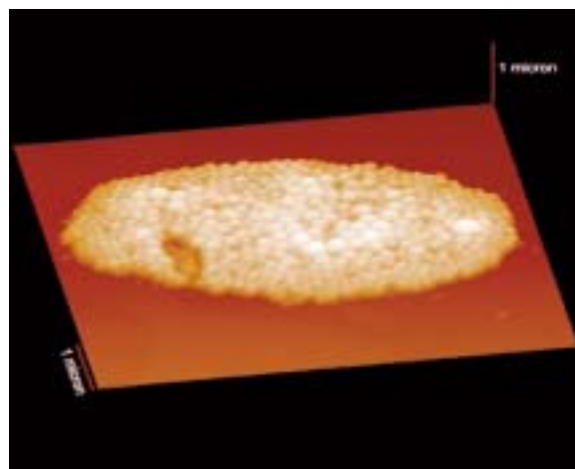


Figure 2. Tapping mode AFM image of *Sepia* eumelanin dried on mica.

sonication and then air-dried on mica. The morphology is similar to that revealed by SEM images of intact granules shown above. There is high salt content in *Sepia* eumelanin. To reduce the salt content, a eumelanin sample was subjected to two cycles of washing (i.e. dispersed in double distilled water, sonicated for 30 minutes in a water bath, centrifuged at 3000 rpm, and discarding the supernatant). The supernatant resulting from a third such washing was collected and air dried on mica. Figure 3 shows an AFM image of the resulting pigment. Unlike Figure 2 there is great uniformity among the constituent structures. In fact, in many locations, a hexagonal closed-pack structure is observed. Thus, after removal of most of the salt and protein fragments, the eumelanin appears to be packed in uniform structures. Previous AFM studies have confirmed these structures are not single polymeric units, establishing the ~ 150 nm structures are comprised of molecular constituents that are small compared to the dimensions of the AFM tip.

To gain more information on the dimensions of these molecular components, images were collected on a molecular weight (MW) fractions isolated using ultrafiltration. Consider the $3000 < \text{MW} < 10000$ fraction. In the preparation of

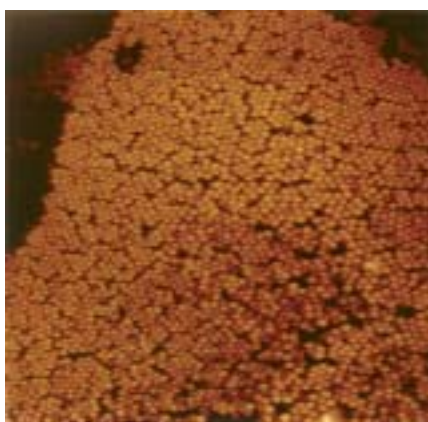


Figure 3. Tapping mode AFM image of dried *Sepia* eumelanin on mica obtained by drying a eumelanin suspension following three cycles of washing. The image is a 7.7 μm x 7.7 μm square region.

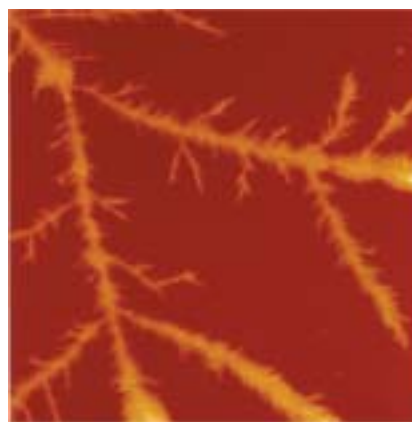


Figure 4. Fractal-like deposit observed upon drying the $1000 < \text{MW} < 300$ fraction of *Sepia* eumelanin on mica. The image is a 20 μm x 17.6 μm region.

this sample, the above ~150 nm structures are destroyed by their passage through the membrane disk under mild N₂ pressure (40 psi). Images of this sample dried on mica reveal fractal-type growth patterns, Figure 4. The growth involves the re- aggregation of small structures, but we do not observe any evidence for the reassembly of the material into ~150 nm structures like those shown in Figure 3. Thus, the ~150 nm structures could not be self-assembled from the constituent oligomers under the conditions used *in vitro*.

The Origin of the Action Spectrum for Oxygen Photoconsumption by Eumelanin

Photochemical excitation of eumelanin can result in the activation of oxygen, the most important primary photochemical pathway being the formation of the superoxide anion, O₂⁻. In an effort to quantify the activation of molecular oxygen by eumelanin, Sarna and coworkers determined the action spectrum for the photoconsumption of oxygen by eumelanin.¹⁷ While eumelanin exhibits absorption throughout the visible and ultraviolet region, photoconsumption only occurs for wavelengths shorter than 400 nm. In their original report Sarna and coworkers suggested that the chromophore responsible for oxygen photoconsumption differed from that which dominated the absorption spectrum.¹⁷ One explanation would be that eumelanin is comprised of a number of molecular entities and one particular constituent has an absorption spectrum matching the action spectrum. Given the above discussion of the structural morphology of the pigment, however, it is reasonable to propose that the molecular basis may be rather homogeneous and that different sized aggregates have different spectroscopic and photoreactive properties. In this case, a specific arrangement of the oligomeric building blocks (individual or aggregated) would be responsible for the photoconsumption of oxygen.

The optical properties of different mass-selected fractions of eumelanin solutions were examined and Figure 5 shows the optical absorption for the MW < 1000 fraction of eumelanin from both *Sepia* and black human hair match the action spectrum for photoconsumption of oxygen.^{18,19} Samples of larger masses (e.g., 1000 < MW < 3000, MW > 10000) exhibit increased absorption at longer wavelengths, and these fractions are currently believed to be aggregates of the oligomers present in the MW < 1000 solution. The absorption spectrum of the MW < 1000 does not extend out to the longer wavelengths exhibited by the spectrum of the bulk pigment. Aggregation results in absorption at longer wavelengths. Photoacoustic studies suggest that the optical density in the visible is dominated by absorption and not light scattering, so association of the eumelanin oligomers results in electronic structure changes in the pigment that broaden the absorption spectrum to lower energy.¹⁹

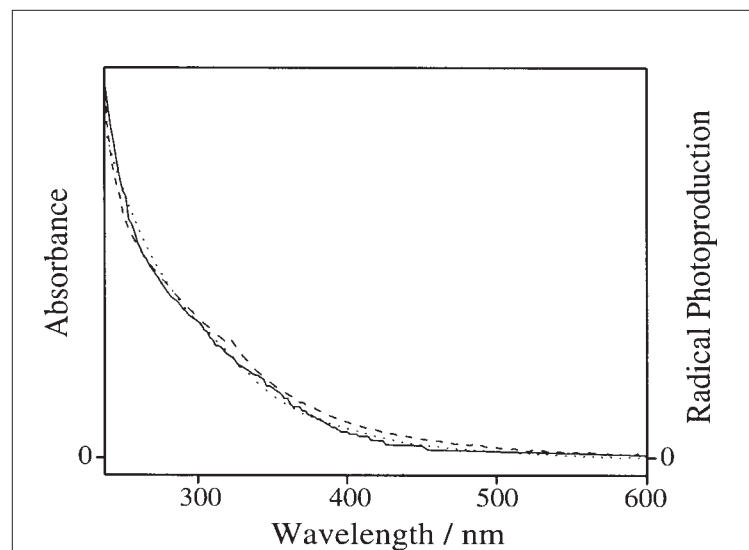


Figure 5. The optical spectra for MW < 1000 fraction of hair eumelanin (dashed), MW < 1000 fractions of *Sepia* eumelanin (dotted) are compared to the action spectrum¹⁷ for the free radical photogeneration by eumelanin (solid). Quantitative agreement is observed.

Photoacoustic calorimetry revealed the MW < 1000 sample is the only mass fraction showing measurable energy storage following UV-A excitation.¹⁹ These data suggest unaggregated oligomers underlie the phototoxic effects of melanin. This prompted a series of optical experiments to probe the photophysical and photochemical behavior of the MW < 1000 fraction. Ultrafast laser experiments showed 90% of the photoexcited molecules relax to the ground state within 20 ps.²⁰ The remaining 10% do not recover on less than the nanosecond time scale, and likely reflect formation of a transient intermediate(s). The presence of intermediate species is confirmed by ESR studies and these intermediates ultimately lead to the consumption of oxygen and production of ROS and free radicals.^{17,21}

Aggregation-Dependent Photogeneration of Superoxide Radical Anion

While the comparison shown in Figure 5 implicates small oligomers as the photoreactive component of melanin, they do not directly inform us whether aggregation affects photoreactivity. It is important to ask how and if aggregation affects the mechanism and yield of ROS photoproduction by

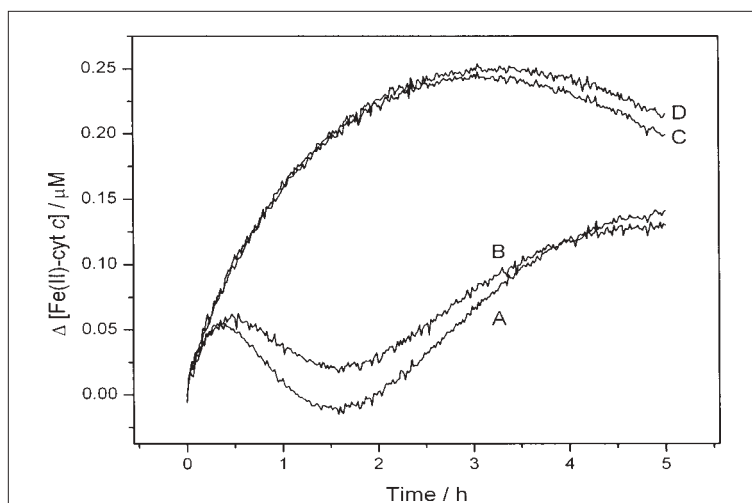


Figure 6. Kinetic traces for the time-dependent changes in Fe(II)-cyt *c* concentration induced by irradiation of MW < 1000 *Sepia* eumelanin at various times following size separation. (A) 0 hrs., eumelanin optical density at 302 nm = 0.040; (B) 17.5 hrs., eumelanin optical density at 302 nm = 0.042; (C) 41.2 hrs.; For both C and D the eumelanin optical density at 302 nm is 0.088; (D) 66.5 hrs.

eumelanin. To address this issue, we examined the kinetics of UV-B (302 nm) induced photoreduction of cytochrome *c* (cyt *c*) by eumelanin.²² Specifically, the kinetics of irradiated solutions of MW < 1000 eumelanin and cyt *c* were performed at various times following generation of the sample. This sample was chosen because we have demonstrated that the constituents of the MW < 1000 sample aggregate slowly over time. Thus, the kinetics could be examined at varying degrees of aggregation. In performing these experiments, it is important to follow the photochemical processes for time periods short in comparison to the time required for the pigment to aggregate.

Figure 6 shows the results for a MW < 1000 sample maintained at room temperature and in the dark for various lengths of time prior to study. Initially, (A) the time course of $\Delta[\text{Fe(II)-cyt } c]$ is quite complicated, reflecting several different chemical events. Studies with selective quenchers show the dynamics originate from the photoproduction of $\text{O}_2^{\cdot -}$. A detailed explanation of the shape of the $\Delta[\text{Fe(II)-cyt } c]$ vs. time plot is beyond the scope of this article, and the reader is referred to our recent report for a complete discussion.²² Herein, we stress what these data reveal with respect to the affect of

aggregation on the redox reactions of melanin with cyt *c*. When solutions of MW < 1000 eumelanin and cyt *c* were incubated at room temperature in the dark for 17.5 h prior to irradiation (B), small effects on both the time course of $\Delta[\text{Fe(II)-cyt } c]$ and the absorption spectrum were observed, indicating that some aggregation had occurred. By 41.2 h after filtration, aggregation had caused the absorption spectrum to broaden to lower energy and increase in intensity in the ultraviolet and near-visible regions. The temporal behavior of $\Delta[\text{Fe(II)-cyt } c]$ had changed drastically (C), becoming similar to that observed for eumelanin stock solutions (data not shown). No more significant changes in the absorption spectrum or $\Delta[\text{Fe(II)-cyt } c]$ kinetics were observed with increased sample storage time, although the absorption spectrum had not fully evolved to that characteristic of bulk eumelanin, for which much more extensive absorption is observed in the visible and near-UV.

Based on the initial slopes of the $\Delta[\text{Fe(II)-cyt } c]$ data in Figure 6, the initial reduction rate of cyt *c* does not change with aggregation. The optical density of the solution increased with time, however, and so the apparent quantum yield for $\text{O}_2^{\cdot -}$ formation decreased as aggregation increased. After 17.5 h, the apparent yield decreased from 7.4×10^{-3} to 4.1×10^{-3} . Examination of the spectrum of bulk eumelanin shows that continued aggregation must broaden the spectrum and increase the absorption at 302 nm. This should result in a further decrease in the apparent quantum efficiency of $\text{O}_2^{\cdot -}$ formation, consistent with the reported values of 6.6×10^{-4} to 1.7×10^{-3} for the bulk pigment.²³ Thus aggregation appears to decrease the efficiency of $\text{O}_2^{\cdot -}$ photoproduction.

Aggregation-Dependent Production of Hydrogen Peroxide

We recently reported the quantum efficiency of hydrogen peroxide, H_2O_2 , production by the MW < 1000 fraction is 5.7×10^{-3} .²² The formation of H_2O_2 is attributed to reaction between $\text{O}_2^{\cdot -}$ and hydroquinone groups on the oligomeric molecules. The quantum yield becomes immeasurable upon aggregation and we speculate this effect is due to a decrease in surface concentration of hydroquinone sites available to react $\text{O}_2^{\cdot -}$ upon pigment aggregation, however, this remains to be established. In any event, aggregation clearly reduces the production of this unwanted oxidant.

Aggregation-dependent generation of reactive oxygen species by eumelanin presents a framework for understanding contrasting photoprotective and phototoxic roles exhibited by eumelanin. The equivalence between the action spectrum and absorption spectrum in Figure 5 along with the aggregation-dependent quantum efficiencies for $\text{O}_2^{\cdot -}$ and

H₂O₂ implicate the oligomers as the phototoxic component. Thus, any changes in melanin that lead to a disruption of the aggregated structure could result in increased oxidative stress. The fact that oligomers generate more H₂O₂ than aggregated pigment may have significant biologic ramifications. H₂O₂ can react with a variety of cellular components, causing for example lipid peroxidation of membrane and hydroxylation of proteins and DNA.²⁴ Such processes may be important in keratinocyte cells, where melanin is deposited as a dust, or in retinal pigment epithelium cells where the structural features of melanosomes are found to change with age, or in pathogenesis of Parkinson's disease where pigmented neurons are more vulnerable and neuromelanin is lost in parallel to neuron degeneration.

Acknowledgements

We thank Susan Forest, Chris Clancy, Emily Weinert, and Tong Ye, for their contributions to this project. This research could not have been done without the financial support of Duke University, the National Institutes of Health, the Lord Foundation, and Unilever Research US. JDS thanks Dr. Tadeusz Sarna for many stimulating discussions about melanins.

References

1. Ito, S. *J. Invest. Dermatol.* **1993**, *100*, S166-S171.
2. Crippa, R.; Horak, V.; Prota, G.; Svoronos, P.; Wolfram, L. In *The Alkaloids*; Brossi, A., Ed.; Academic Press, Inc., 1989; Vol. 36, pp 253-323.
3. Zeise, L.; Chedekel, M. R.; Fitzpatrick, T. B., Eds. *Melanin: Its role in human photoprotection*; Valdmnar Press; 1995.
4. Pezzella, A.; Napolitano, A.; d'Ischia, M.; Prota, G.; Seraglia, R.; Traldi, P. *Rapid Commun. Mass Spectrom.* **1997**, *11*, 368-372.
5. Cheng, J.; Moss, S. C.; Eisner, M. *Pigm. Cell. Res.* **1994**, *7*, 263-273.
6. Cheng, J.; Moss, S. C.; Eisner, M.; Zschack, P. *Pigm. Cell. Res.* **1994**, *7*, 255-262.
7. Gallas, J. M.; Littrell, K. C.; Seifert, S.; Zajac, G. W.; Thiyagarajan, P. *Biophys. J.* **1999**, *77*, 1135-1142.
8. Zajac, G. W.; Gallas, J. M.; Alvaradoswaisgood, A. E. *J. Vac. Sci. Technol. B* **1994**, *12*, 1512-1516.
9. Zajac, G. W.; Gallas, J. M.; Cheng, J.; Eisner, M.; Moss, S. C.; Alvaradoswaisgood, A. E. *Biochim. Biophys. Acta-Gen. Subj.* **1994**, *1199*, 271-278.
10. Gallas, J. M.; Zajac, G. W.; Sarna, T.; Stotter, P. L. *Pigm. Cell. Res.* **2000**, *13*, 99-108.
11. Clancy, C. M. R.; Nofsinger, J. B.; Hanks, R. K.; Simon, J. D. *J. Phys. Chem. B* **2000**, *104*, 7871-7873.
12. Clancy, C. M. R.; Simon, J. D. *Biochemistry* **2001**, *40*, 13353-13360.
13. Nofsinger, J. B.; Forest, S. E.; Eibest, L. M.; Gold, K. A.; Simon, J. D. *Pigm. Cell. Res.* **2000**, *13*, 179-184.
14. Zeise, L.; Addison, R. B.; Chedekel, M. R. *Pigm. Cell. Res.* **1992**, 48-53.
15. Zeise, L.; Murr, B. L.; Chedekel, M. R. *Pigm. Cell. Res.* **1992**, *5*, 132-142.
16. Hill, H. Z. *Bioessays* **1992**, *14*, 49-56.
17. Sarna, T.; Sealy, R. C. *Arch. Biochem. Biophys.* **1984**, *232*, 574-578.
18. Nofsinger, J. B.; Weinert, E. E.; Simon, J. D. *Biospectroscopy* **2002**, in press.
19. Nofsinger, J. B.; Forest, S. E.; Simon, J. D. *J. Phys. Chem. B* **1999**, *103*, 11428-11432.
20. Nofsinger, J. B.; Ye, T.; Simon, J. D. *J. Phys. Chem. B* **2001**, *105*, 2864-2866.
21. Sarna, T.; Sealy, R. C. *Photochem. Photobiol.* **1984**, *39*, 69-74.
22. Nofsinger, J. B.; Liu, Y.; Simon, J. D. *Free Radic. Biol. Med.* **2002**, in press.
23. Sarna, T.; Menon, I. A.; Sealy, R. C. *Photochem. Photobiol.* **1984**, *39*, 805-809.
24. Symons, M. C. R.; Rusakiewicz, S.; Rees, R. C.; Ahmad, S. I. *Med. Hypotheses* **2001**, *57*, 56-58.

About the Authors

John D. Simon is the George B. Geller Professor and Chairman of the Department of Chemistry, Duke University, Durham, North Carolina 27708. His group is currently studying the structure photochemistry of pigments (melanin, ocular lipofuscin), and the interaction between ochratoxin A and proteins in human blood plasma.

Yan Liu received her Ph.D. from Columbia University in 2000. After a one year postdoctoral research at The Rockefeller University doing photobiology, she was appointed as a research associate at Duke University. Her research interests are in spectral and structural analyses of biopigments.

Brian Nofsinger received his Ph.D. from Duke University in 2001 for his work on the spatial and temporal properties of eumelanins.

Light-Based Detection Systems in Modern Gas Chromatography

Thomas G. Chasteen, Department of Chemistry, Sam Houston State University

Chromatography: The Science of Separation

The advent of higher and higher resolving gas chromatographic systems has led to a revolution in the analysis of volatile chemical compounds. Gas chromatography (GC) is a method of separating a mixture of compounds, often termed analytes, into individual components using their chemical/physical differences. A mixture of analytes to be separated is introduced onto a GC column (a long, small diameter tube most often coated with specialized material on the inner wall's surface) in the form of a gas. Differential interactions between the analytes and the column cause different analyte molecules to separate in space as they pass through the column. Components introduced at the column's head as a mixture come off the column's end one by one. This is called elution.

Samples that were once considered to contain only a few individual compounds, when analyzed by early GC systems, have yielded tens or hundreds of compounds when analyzed by higher and higher resolving GC columns. This is because compounds which previously eluted from a GC column simultaneously are now completely separated and appear as multiple peaks on the data output of the GC process called a chromatogram. Figure 1 is an example of two chromatograms stacked one on top of the other for comparison. The horizontal axis is time and the vertical is (electronic) detector signal (see below).

Detection in Gas Chromatography

After separation by GC, analytes still need to be detected as they exit the column and therein lies the wonderful world of GC detectors. Photochemical or spectrochemical detectors play a strong role because they allow sensitive detection—that is excellent detection limits or selectivity. That is, they offer the power to determine one analyte in the presence of other interfering compounds.

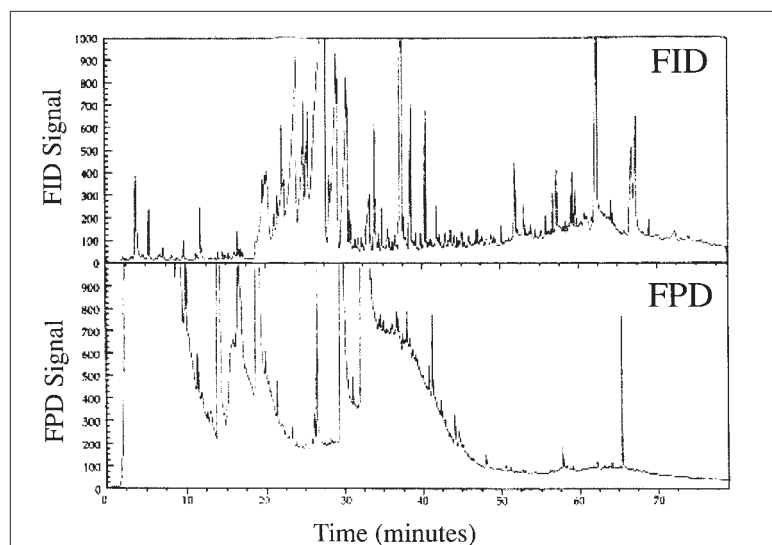


Figure 1. Two chromatograms of the same chemical mixture analyzed with two different GC detectors. Top is an FID chromatogram; bottom is an FPD chromatogram. (Reprinted from *Agricultural and Forest Meteorology*, Vol 108, Schiffman Bennett, and Raymer, Pages No. 213-240, Copyright 2001, with permission of Elsevier Science.)

The job of the GC detector is to determine exactly when a compound exits the column and to provide an electronic signal proportional to the quantity of that analyte's peak. The elution time of a chromatographic analyte is formally called the retention time. The detector signal intensity of an analyte is compared to that of a known amount of a standard, and this process allows the chromatographer to quantify the amount of the known compounds.

The reason to use more than one kind of detector for gas chromatography is to achieve selective and/or highly sensitive detection of specific compounds encountered in particular chromatographic analyses. The workhorse GC detector is the flame ionization detector (FID). This device is configured so that the end of the GC column is plumbed directly into a hydrogen/air flame jet which, in effect, burns the column's analytes as they exit the column and generates a signal that stems from those compounds' ions produced in the flame. The energy of the flame is not enough to completely atomize samples, but instead

produces ionized molecular fragments. The FID is very sensitive to molecules that contain carbon and hydrogen atoms (hydrocarbons). GCs using FIDs are therefore widespread in the petrochemical industry (Na et al., 2001; Hernández-Beltrán et al., 2001); however, the presence of other kinds of atoms (so called heteroatoms) in analyte molecules degrades the signal the FID produces so other kinds of detectors are also needed.

Photochemical Detectors in GC

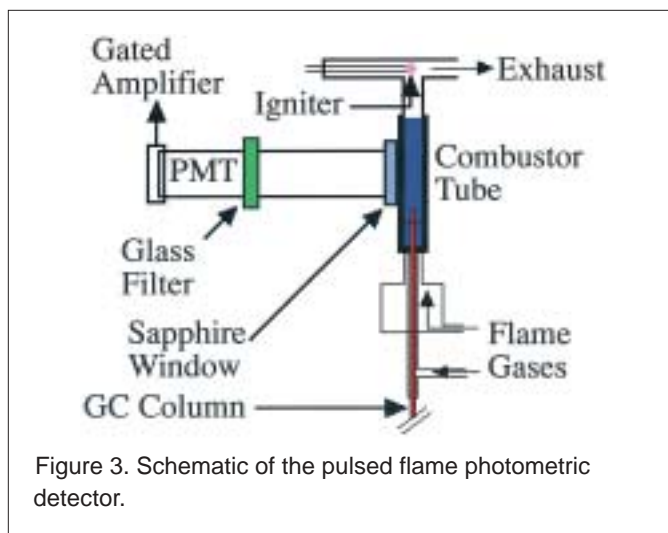
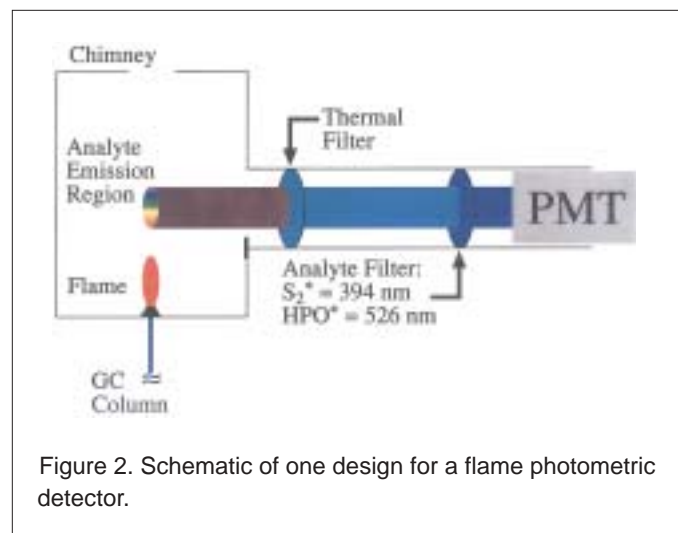
The determination of sulfur or phosphorus containing compounds is the job of the flame photometric detector (FPD) one of the earliest photochemical GC detectors (Brody and Chaney, 1966). This device uses the chemiluminescent reactions of these compounds in a H_2 /air flame as a source of analytical information that is relatively specific for substances containing these two kinds of atoms. Instead of responding to ions like the FID, the source of the FPD's signal is from the light produced by an excited molecule created in the flame's combustion, that is, a photochemical process called chemiluminescence. The light emitting species for sulfur compounds is an excited S_2 fragment created in the flame (commonly noted as S_2^*). The maximum light emission of S_2^* is approximately 394 nm. (Again molecular fragments are the signal producers.) The emitter from reacting phosphorus compounds in the FPD flame is excited HPO^* (light emission centered around 510-526 nm). In order to selectively detect one or the other family of compounds as it elutes from the GC column, an interference filter is used between the flame and the photomultiplier tube (PMT) to isolate the appropriate emission band. The drawback here is that the filter must be exchanged between chromatographic runs if the other family of compounds is to be detected or two different PMTs and filters must be built into the design. Figure 2 is a drawing/schematic of the FPD. The bottom chromatogram in Figure 1 comes from the same chemical sample as the top chromatogram in that figure but analyzed with the FPD instead of the FID. The fact that some analytes show up in one detector's chromatogram and not the other is an excellent example of detector selectivity. If the analyst is interested in sulfur compounds in swine factory emissions the bottom chromatogram is the key; otherwise the FID chromatogram shows the sample's hydrocarbons (Schiffman et al., 2001).

In addition to the instrumental requirements for 1) a combustion chamber to house the FPD's flame, 2) gas lines for hydrogen (fuel) and air (oxidant), and 3) an exhaust chimney to remove combustion products, the final component necessary for this instrument is a thermal (bandpass) filter to isolate only the visible and UV radiation emitted by the flame.

Because many different kinds of atoms emit light in this type of flame, the photochemical processes of the FPD have been applied to compounds containing S, P, Se, Ge and Ru with varying amounts of success (Aue and Singh, 2001). FPDs find application in pesticides, derivatized blister agents, and sulfur emissions from animal wastes (Tompkins et al., 2001; Yao et al., 2001; Schiffman et al., 2001). Other GC detectors also find uses in gas chromatography.

Pulsed Flame Photometric Detector (PFPD)

The pulsed flame photometric detector (PFPD) is a relatively new weapon in the arsenal of the analytical chemist (Amirav and Jing, 1995; Jing and Amirav, 1997). Though it uses a flame like the FPD, the PFPD is a significant improvement because it can provide better sensitivity and selectivity for sulfur and phosphorus. The old FPD was



generally only used for sulfur and phosphorus and a few others (see page 8); however, the PFPD allows for selective detection of S and P primarily but also detects compounds containing many other heteroatom-containing species as well by using software processing of the PMT's signal.

As this instrument's schematic diagram shows on page 8, the PFPD has a combustion chamber (or combustor tube) like the old FPD and a PMT like the FPD. However in this new detector, two different combustible gas flows enter the bottom of the combustion chamber through narrow gas lines. The normal FPD has only one fuel line which is for hydrogen. It also has air plumbed in. The second incoming gas flow's job in the PFPD is to help fill up the outer volume of the combustion chamber, and outside the combustion zone which is in the center of the combustion tube, while the analyte and the primary combustion gas flow into that chamber. The capillary gas chromatographic column from the GC oven enters at the bottom of the combustor (also like the FPD).

At the top of the PFPD is an ignition wire which stays continuously red hot. When the gases flowing into the combustor, including the analytes exiting the GC column, reach a flammable mixture they are ignited by the ignition wire; the flame ignites at that wire and propagates back down the combustor. Here is another big difference between the pulsed flame photometric detector and the old FPD: The flame front terminates, that is, uses up all of the quickest burning flammable material in the combustor in less than 10 milliseconds and the flame goes out. It is AFTER this short flame pulse that the slower burning analytes are excited and emit the light that is characteristic of their elements. Therefore, it is also during this period that the PMT, in a manner similar to the old FPD, records the analyte's light from the combustion chamber. After about 300 milliseconds, the flame pulses again as new flammable material fills the combustion chamber from the inlet tubes and GC column. That combination once again constitutes a flammable mixture. In this way about three flame pulses are recorded per second.

Here's where the PFPD's selectivity arises. The shape of the flame pulse profile, over time, depends on the elements in the analytes that are present in the flame. The temporal light emissions are characteristic of whichever chemical analyte is eluting from the GC column; some emit faster and some slower. Using this information the PFPD can be used to determine compounds containing many, many different elements: N, As, Sn, Se, Ge, Te, Sb, Br, Ga, In and Cu among others (Amirav and Jing, 1995).

Photoionization Detector (PID)

The selective determination of aromatic hydrocarbons or organo-heteroatom species is the job of the photoionization detector (PID). This device, also about as old as the FPD (Price et al., 1968), uses ultraviolet light as a means of ionizing an analyte exiting from a GC column. While the energy of this process is even less than the flames of the FID or FPD, the analyte molecules are still ionized and the ions produced by this process are collected by electrodes. The electrode current generated is therefore a measure of the analyte concentration.

If the energy of an incoming photon is high enough (and the molecule's electrons are quantum mechanically "allowed" to absorb the photon) photo-excitation can occur to such an extent that an electron is completely removed from its molecular orbital, i.e. ionization.

If the amount of ionization is reproducible for a given compound, pressure, and light source then the current collected at the PID's reaction cell electrodes is reproducibly proportional to the amount of that compound entering the cell. The reason why the compounds that are routinely analyzed are either aromatic hydrocarbons or heteroatom containing compounds (like organonitrogen or organophosphorus species) is because these species have ionization potentials (IP) that are within reach of commercially available UV lamps. The available commercial lamp energies range from 8.3 to 11.7 eV, that is, lambda max ranging from 150 nm to 106 nm. Although most PIDs have only one lamp, lamps in the PID can be exchanged depending on the compound selectivity required in the analysis.

Here is an example of selective PID detection: Benzene's boiling point is 80.1 degrees C and its IP is 9.24 eV. This compound would respond in a PID with a UV lamp of 9.5 eV because this lamp's photon's energy is higher than benzene's IP (9.24). Isopropyl alcohol has a similar boiling point (82.5 degrees C); these two compounds might elute relatively close together in normal temperature programmed gas chromatography, especially if a fast temperature ramp were used. However, since isopropyl alcohol's IP is 10.15 eV this compound would be invisible or show very poor response in that PID (that is, configured with that lamp), and therefore the detector would respond to one compound but not the other. That is, only benzene would produce a chromatographic peak even if isopropyl alcohol were present.

Very recent PID applications have involved the determination of derivatized hydrides of arsenic collected in the western Atlantic Ocean (Cutter et al., 2001) and chemical warfare agents (Suryanarayana et al., 2001).

Atomic Emission Detector (AED)

Since more and more complex chemical mixtures can be successfully separated, subsequent gas chromatograms are increasingly more complex. Therefore, the need to differentiate between the sample components using the GC detector as a means of compound discrimination is more and more common. One of the newest additions to the gas chromatographer's toolkit is the atomic emission detector (AED). This detector, while quite expensive compared to other commercially available GC detectors, is an extremely powerful alternative. For instance, instead of measuring simple gas phase (carbon containing) ions created in a flame as with the flame ionization detector or the emission from sulfur or phosphorus species in the flame photometric detector, the AED has a much wider applicability because it is based on the detection of atomic light emissions. If light from its plasma is divided into individual atomic emission lines using a light separating device called a monochromator, then information can be gained about the atomic make-up of each different analyte in a sample (Quimby and Sullivan, 1990).

As analytes come off the capillary column they are fed into a microwave powered plasma (or discharge) cavity where the compounds' bonds are completely destroyed and their atoms are excited by the energy of the plasma, energy that is much higher than that of the flame systems discussed above. The light that is emitted by the excited atoms is separated into individual emission lines via an optical grating and the lines shined onto a photodiode array. The photodiode array can simplistically be thought of as hundreds of different PMT grouped together with

each individual diode converting light into electrical signals. The associated computer then sorts out the individual emission lines and can produce chromatograms made up of peaks from analytes that contain only a specific element.

The components of the AED include: 1) an interface for the incoming capillary GC column to the microwave induced plasma chamber; 2) the microwave chamber itself; 3) a cooling system for that chamber; 4) a diffraction grating and associated optics to focus then disperse the spectral atomic lines; and 5) a position adjustable photodiode array interfaced to a computer. The microwave cavity cooling is required because much of the energy focused into the cavity is converted to heat.

Instead of plotting chromatograms based solely on the total signal from the detector, the AED can produce element-specific chromatograms: a plot like that of Figure 1 but only showing chromatographic peaks of analytes con-

taining, for instance, nitrogen or selenium atoms; and with software/signal manipulation, chromatograms for each subject element can be generated. Because of this sort of ultimate selectivity, this is a very powerful detector. AEDs find applications in coal analysis (Ross et al., 2001) and difficult to analyze alkylphenols compounds following chemical derivatization (Rolfes and Andersson, 2001).

Summary

The power of photochemical GC detectors gives the chemical analyst the ability to detect very low concentrations of important analytes alone or in the presence of high concentration of interferants even if strict chromatographic separation is not possible. If a compound is thermally stable, that is, will vaporize without decomposition, and has a low enough boiling point, GC with specialized detection is the most chemically powerful analytical method known.

Bibliography

- Amirav, A. and H. Jing. 1995. Pulsed Flame Photometric Detector for Gas Chromatography. *Anal. Chem.* **67**:3305-3318.
- Aue, W. A. and H. Singh. 2001. Chemiluminescent photon yields measured in the flame photometric detector on chromatographic peaks containing sulfur, phosphorus, manganese, ruthenium, iron or selenium; *Spectrochim. Acta Part B.* **56**:517-525.
- Brody, S. S. and J. E. Chaney. 1966. Flame Photometric Detector. *J. Gas Chromatogr.* **4**(2):42-46.

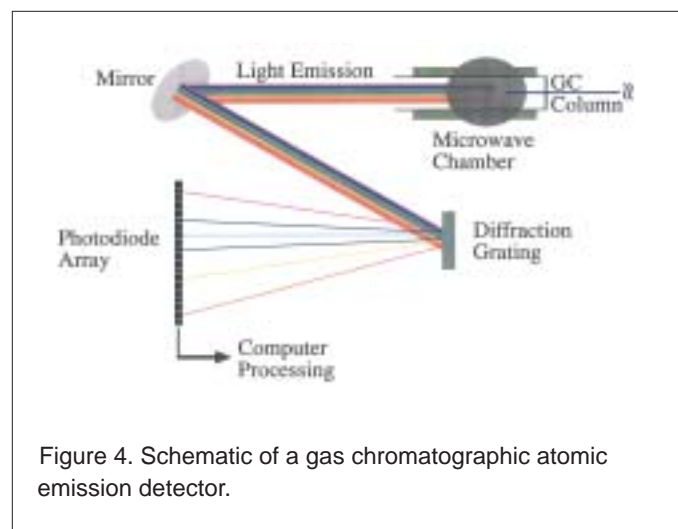


Figure 4. Schematic of a gas chromatographic atomic emission detector.

- Cutter, G. A., L. S. Cuttera, A. M. Featherstone and S. E. Lohrenz. 2001. Antimony and arsenic biogeochemistry in the western Atlantic Ocean; *Deep Sea Res. Part II.* **48**:2895-2915.
- Hernández-Beltrán, F., J. C. Moreno-Mayorga, R. Quintana-Solórzano, J. Sánchez-Valente, F. Pedraza-Archila and M. Pérez-Luna. 2001. Sulfur reduction in cracked naphtha by a commercial additive: effect of feed and catalyst properties. *Appl. Catalysis B.* **34**(2):137-148
- Jing, H., and A. Amirav. 1998. Pulsed Flame Photometric Detector-A Step Forwards Towards Universal Heteroatom Selective Detection. *J. Chromatogr. A.* **805**:177-215.
- Na, K., Yong Pyo Kim, K.-C. Moon, I. Moon and K. Fung. 2001. Concentrations of volatile organic compounds in an industrial area of Korea. *Atmos. Environ.* **35**:2747-2756.
- Price, J. G. W., D. C. Fenimore, P. G. Simmonds, and A. Flatkis. 1968. Design and Operation of a Photoionization Detector for Gas Chromatography. *Anal. Chem.* **40**:541-547.
- Quimby, B. D. and J. J. Sullivan. 1990. Evaluation of a Microwave Cavity, Discharge Tube, and Gas Flow System for Combined Gas Chromatography-Atomic Emission Detection. *Anal. Chem.* **62**:1027-1034.
- Rolfes, J. and J. T. Andersson. 2001. Determination of Alkylphenols after Derivatization to Ferrocenecarboxylic Acid Esters with Gas Chromatography-Atomic Emission Detection. *Anal. Chem.* **73**:3073-3082.
- Ross, A. B., S. Junyapoon, K. D. Bartle, J. M. Jones and A. Williams. 2001. Development of pyrolysis-GC with selective detection: coupling of pyrolysis-GC to atomic emission detection (py-GC-AED). *J. Anal. Appl. Pyrolysis.* **58-59**:371-385.
- Schiffman, S. S., J. L. Bennetta and J. H. Raymerb. 2001. Quantification of odors and odorants from swine operations in North Carolina. *Agric. Forest Meteorol.* **108**:213-240.
- Suryanarayana, M. V. S., R. K. Shrivastava, D. Pandey, R. Vaidyanathaswamy, S. Mahajan and D. Bhoumik. 2001. Simple time weighted average level air-monitoring method for sulfur mustard inwork places. *J. Chromatogr. A.* **907**:229-234.
- Tomkins, B. A., G. A. Sega, and C.-H. Ho. 2001. Determination of Lewisite oxide in soil using solid-phase microextraction followed by gas chromatography with flame photometric or mass spectrometric detection. *J. Chromatogr. A.* **909**:13-28.
- Yao, Z.-W., G.-B. Jiang, J.-M. Liu and W. Cheng. 2001. Application of solid-phase microextraction for the determination of organophosphorous pesticides in aqueous samples by gas chromatography with flame photometric detector. *Talanta.* **55**:807-814.

About the Author

Dr. Thomas G. Chasteen received his Ph.D. in chemistry at the University of Colorado, Boulder. He is currently an associate professor of chemistry at Sam Houston State University. His home page is: www.shsu.edu/~chm_tgc.

Copyright 2002 by the Center for Photochemical Sciences
The Spectrum is a quarterly publication of the Center for
 Photochemical Sciences, Bowling Green State University,
 Bowling Green, OH 43403.
 Phone 419-372-2033 Fax 419-372-0366
 Email photochemical@listproc.bgsu.edu
 WWW <http://www.bgsu.edu/departments/photochem/>

Executive Director: D. C. Neckers
 Principal Faculty: P. Anzenbacher, G. S. Bullerjahn,
 J. R. Cable, F. N. Castellano,
 M. E. Geusz, D. C. Neckers,
 M. Y. Ogawa, V. V. Popik,
 M. A. J. Rodgers, D. L. Snavely,
 B. R. Ullrich
The Spectrum Editor: Pat Green
 Production Editor: Alita Frater

COPYRIGHT PERMISSION

A person may make a single copy of any or all articles in this issue for personal use. Copying beyond that permitted by the U.S. Copyright law is allowed provided that the appropriate per copy fee is paid through the Copyright Clearance Center, Inc., 27 Congress St., Salem, MA 01970. For reprint permission, please write to the Center for Photochemical Sciences.

EDITORIAL POLICY

The Spectrum reserves the right to review and edit all submissions. The Spectrum is not responsible for contents of articles.

Articles submitted to The Spectrum will appear at the discretion of the editorial staff as space is available.

Bistable Optoelectronic Device Realization by Photocurrent Bleaching

Bruno Ullrich, Centers for Materials and Photochemical Sciences,
Department of Physics and Astronomy, Bowling Green State University

Optoelectronic bistability is observed in a CdS single crystal by bleaching of an alternating photocurrent by a continuous wave optical bias. Exploitation of lock-in technique produces a bistable switch. The hybrid device requires extremely low electric fields ($1\text{-}2\text{ V cm}^{-1}$), and highly sensitive optoelectronic links and hybrid survey applications seem feasible with the introduced device concept.

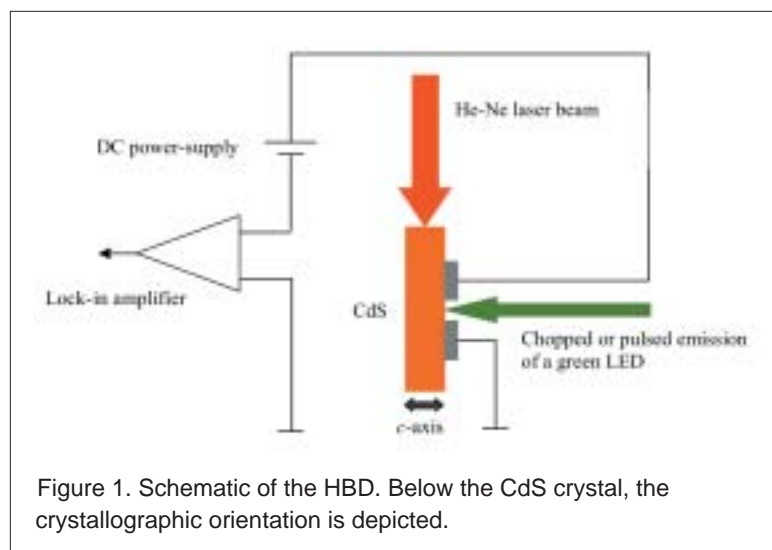
Introduction

Although all-optical technologies for data transfer appear feasible, the reality is that electronic conversion will continue to dominate optical networks for quite some time.¹ The problem with the fully optical approach is that photonic switches are not commercially available in the required size and density to meet the technical requirements to fully replace or even surpass standard electronics. On the other hand, due to the increasing demand for telecommunications and data-storage capacity, it is clear that any foreseeable future development in the field of data processing requires enhanced optical routing of signals.²

An optoelectronic hybrid device merges optical switching concepts with an electronic core to yield a smart progeny that will provide a seamless upgrade path to a pure photonic switch architecture in the future.¹ Therefore, it is desirable that hybrid switch design merges the best of both the electrical and photonic technologies. It seems, however, that hybrid concepts are far from being exhaustively studied. A sophisticated, but nevertheless very well known and reliable concept, lock-in technique is usually used in metrology rather than the realization of optoelectronic switches. In this paper, it is demonstrated that the lock-in concept in conjunction with a photoconductor is very useful for the achievement of hybrid bistable devices (HBDs).

Device Concept

Figure 1 shows the HBD.^{3,4} The photoconductor used is an industrially produced Cadmium Sulfide (CdS) crystal from the gas phase with a cross-section of $2\times 2\text{ mm}$ and a length of 9 mm . The electrical connection is performed by evaporated Indium contacts, which are separated by 1 mm . A commercial green ($\approx 520\text{ nm}$) light emitting diode (LED) illuminates the crystal. The emission of the LED is chopped at 278 Hz , providing the reference frequency for the lock-in amplifier. Due to an applied constant electric field, the chopped LED illumination causes an alternating photocurrent (APC), which is detected with a lock-in amplifier. So far, the arrangement is identical to standard photocurrent



measurements employing lock-in technique. The difference from standard experiments is that the CdS crystal is additionally illuminated at 1.96 eV employing a He-Ne laser. The crystal weakly absorbs the irradiation of the He-Ne laser since the gap of CdS is at 2.45 eV . The intensity of the laser beam is swept in the mHz-Hz range by means of a liquid-crystal light control system. This represents, in comparison to the LED, a non-modulated continuous wave (cw) excitation, which causes direct photocurrent (DPC) in the crystal. By measuring the impinging power of the He-Ne laser, the setup in Figure 1 is used to record the APC vs. laser intensity. Figures 2 (a) and 2 (b) show the results. At 1 V cm^{-1} , the APC does not show any

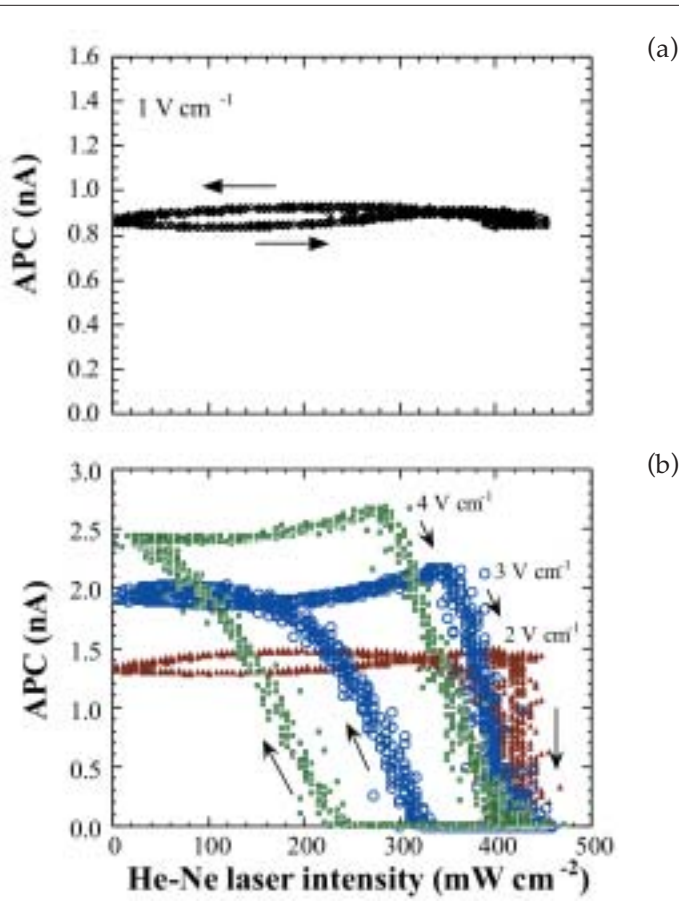


Figure 2. (a) APC vs. intensity of the He-Ne laser at 1 V cm^{-1} . (b) Bistability of the HBD at 2, 3 and 4 V cm^{-1} . The measurements are carried out at 300 K.

noteworthy dependence on the He-Ne laser intensity. The situation is drastically changed at 2 V cm^{-1} , where the APC exhibits a bistable switch practically without hysteresis. An increase of the electric field produces hysteresis and reduces the intensity necessary to evoke switching. This behavior is known from thermo-optical hybrid logic gates formed with thin film CdS.⁵ Part of the switching energy is delivered by the bias by lowering the required optical power.

Discussion of the Device Function

In order to explain the bistable switch, one has to consider the different currents in the crystal, i.e., APC, DPC and dark DC current. The latter, exceeds the APC by five orders of magnitude at the voltages in Figure 2 since the dark resistance of the crystal between the contacts is only 598Ω . Hence, the switching of the HBD in Figure 2 (b) is understood by the bleaching of the APC, which is mainly generated in the surface region of the crystal, by the DPC due to the bulk penetrating cw illumination of the He-Ne laser in addition to the dark DC current at a certain electric field. It has been pointed out previously⁶ that a critical electron concentration of $n_c \approx 10^{18} \text{ cm}^{-3}$ prevents the build up of APC in thin film CdS under moderate illumination since the sample appears to be too “metallic” and the electron concentration remains untouched by light. Hence, considering the low He-Ne laser intensity and the small voltages required to induce the bistable switch, the dark con-

centration of the crystal should be close to the critical value. In order to check this, we excited the crystal between the contacts with the He-Ne laser. The dark concentration n_d is found with the following relation,

$$n_d = \frac{I_0 \tau (R_i / R_d) (1 - \exp(-\alpha d))}{(h\nu) d (1 - R_i / R_d)} \quad (1)$$

where, I_0 is the incident He-Ne laser intensity, τ is the lifetime of the excited electrons, R_i is the resistance of the crystal under illumination, R_d ($=598 \Omega$) the dark resistance, α is the absorption constant, d is the thickness of the crystal ($=0.2 \text{ cm}$), and $h\nu$ ($=1.96 \text{ eV}$) the photon energy. For $I_0=320 \text{ mW cm}^{-2}$, we find $R_i=555 \Omega$. The lifetime is measured via the photocurrent decay employing a 500 MHz oscilloscope. The decay is shown in Figure 3 and the exponential fit of the data gives $\tau=22 \text{ ms}$. Transmittance studies at 1.96 eV show that $\alpha \approx 1 \text{ cm}^{-1}$. With these parameters, we find $n_d=3 \times 10^{17} \text{ cm}^{-3}$, which is indeed fairly close to the critical concentration.

So far, basically, the optoelectronic behavior of the sample is represented by the circuit of two parallel resistances. One resistance, which is constant, draws the APC, and the other becomes less due to the illumination resulting finally in an electric shorting of the constant resistance. There are, however, several additional properties to consider in order to fully comprehend the function of the device. In spite of the weak intensity, the He-Ne laser causes incoherent two-photon processes.⁷ Therefore, we believe, that the DC shorting takes place not only via impurity states directly excited by the He-Ne laser emission, but also by electrons excited into the conduction band. Such a process eventually explains the sharp switching threshold at 2 V cm^{-1} in Figure 2 (b). Currently, additional experiments are being conducted to explore the influence of two-photon processes on the switching characteristic of the HBD.

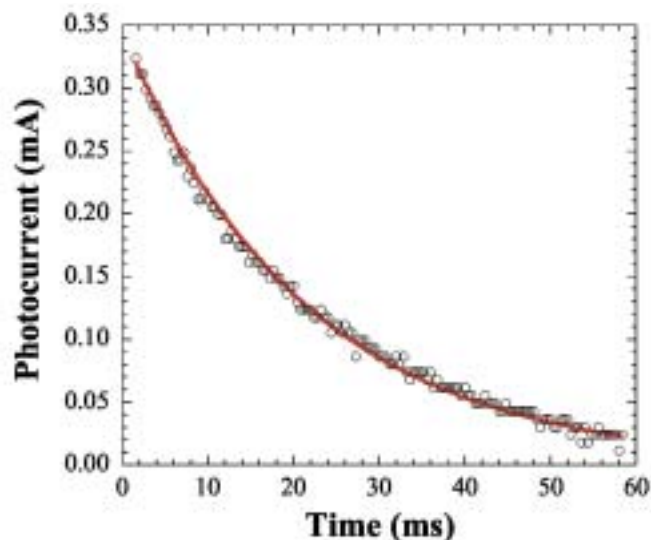


Figure 3: Decay of the photocurrent evoked with He-Ne laser irradiation. The measurement was performed at 300 K with an applied electric field of 30V cm^{-1} . The solid line represents the exponential fit of the data.

Comparison With Other Concepts

It is important to compare the HBD presented with already existing optoelectronic devices. The most common is the use of photodiodes to achieve optoelectronic switches.⁸ Furthermore, during the last 15 years, the so-called self-electrooptic-effect device (SEED)⁹ gained considerable importance in the field. The principle of the device is subject to the quantum-confined Stark effect in a multiple quantum well. It seems that the HBD here has two advantages: a) Most straightforward material requirements, i.e., no specific doping processes or rather complicated and expensive growth methods as molecular beam epitaxy are necessary to form the core of the device. b) The extreme bias sensitivity appears to be unbeatable. Figure 2 demonstrates that an applied voltage of 0.2 V causes the bistable switch. By reducing the contact distance to $1\ \mu\text{m}$, the required voltage is subtle $200\ \mu\text{V}$! As far as this author knows such switching sensitivities are extremely difficult to achieve with the aforementioned known concepts.

Conclusion

A novel optoelectronic bistable device is demonstrated by the superposition of two light beams in an electrically biased CdS crystal. One of the irradiations is used as optical cw bias below the gap bleaching the alternating photocurrent signal excited at the gap with a chopped light source. The bleaching is measured by employing a lock-in technique. The device is capable of switching at extremely low voltage and electric field variations and is of appreciable interest for highly sensitive optically interfaced electronic conversions supplied by low voltage sources, as e.g. piezoelectric crystals.

References

1. Mackey, R. *Lightwave*, June 2001 Supplement.
2. Midwinter, J. E. In *Photonics in Switching*; Midwinter, J. E., Ed.; Academic Press, Inc.: San Diego, 1993; Vol. I, p 1.
3. Ullrich, B. Patent AT 407.445.
4. Ullrich, B.; Dushkina, N. M.; Kobayashi, T. *Proceedings of the International Pacific Rim Conference on Lasers and Electro-Optics*, Makuhari, Japan, 1997, p 311.
5. Ullrich, B.; Bouchenaki, C.; Roth, S. *Appl. Phys. A* **1991**, *53*, 539.
6. Ullrich, B.; Sakai, H.; Segawa, Y. *Thin Solid Films* **2001**, *385*, 220.
7. Ullrich, B.; Dushkina, N. M.; Kobayashi, T. *Jpn. J. Appl. Phys.* **1997**, *36*, L682.
8. MacDonald, R. I. In *Photonics in Switching*; Midwinter, J. E., Ed.; Academic Press, Inc.: San Diego, 1993; Vol. I, p 169.
9. Lentine, A. L.; Miller, D. A. B. *IEEE J. Quantum Electron.* **1993**, *29*, 655.

About the Author

Bruno Ullrich received his Ph.D. degree in Physics from The University of Vienna in 1988. He has held positions at the University of Strasbourg (France), the Technical University of Graz (Austria), The University of Tokyo, and the Institute of Physical and Chemical Research (RIKEN) in Sendai (Japan). In 2000, he joined the Department of Physics and Astronomy at Bowling Green State University. His current research interests include ultra-fast spectroscopy and nonlinear optics on inorganic and organic semiconductors and laser ablation of thin semiconducting films. His mailing address is Department of Physics and Astronomy, Bowling Green State University, Bowling Green, Ohio 43403 and his e-mail address is bruno@kottan-labs.bgsu.edu.

Center for Photochemical Sciences Publications

427. Hoostal, M.; **Bullerjahn, G. S.**; McKay, R. M. L. Development of a PCR-based assay for PCB bioremediation in aquatic sediments. *Hydrobiologia* **2002**, 468.
428. Jarikov, V. V.; **Neckers, D. C.** Photochemistry and photophysics of triarylmethane dye leuconitriles. *J. Org. Chem.* **2001**, 66, 659-671.
429. Fedorov, A. V.; Danilov, E. O.; **Rodgers, M. A. J.**; **Neckers, D. C.** Time-resolved step-scan fourier transform infrared spectroscopy of alkyl phenylglyoxylates. *J. Am. Chem. Soc.* **2001**, 123, 5136-5137.
430. Kaafarani, B. R.; **Neckers, D. C.** Photocyclization of a conjugated triaryl 'Y-enyne'. *Tetrahedron Lett.* **2001**, 42, 4099-4102.
432. Strehmel, B.; Henbest, K. B.; Sarker, A. M.; Malpert, J. H.; Chen, D. Y.; **Neckers, D. C.**; **Rodgers, M. A. J.** Ion-induced manipulation of photochemical pathways in crown ether compounds based on fluorinated oligophenylenevinyls: The border between ultrafast photoswitches and photoproduced nanomaterials. *J. Nanosci. Nanotech.* **2001**, 1, 107-124.
434. **Ullrich, B.**; Schroeder, R.; Graupner, W.; Sakaid, H. The influence of self absorption on the photoluminescence of thin film CdS demonstrated by two-photon absorption. *Optics Express* **2001**, 9, 116.
435. Carney, J. R.; Fedorov, A. V.; **Cable, J. R.**; Zwieter, T. S. Infrared spectroscopy of H-bonded bridges stretched across the cis-amide group: I. Water bridges. *J. Phys. Chem. A* **2001**, 105 (14), 3487-3497.
436. **Cable, J. R.**; Carney, J. R.; Zwieter, T. S. Infrared spectroscopy of H-bonded bridges stretched across the cis-amide group: II. Ammonia and mixed ammonia/water bridges. *J. Phys. Chem. A* **2001**, 105 (35), 8162-8175.
437. Ren, K.; Malpert, J. H.; Li, H.; Gu, H.; **Neckers, D. C.** Studies of weakly coordinating anions paired with iodonium cations. *Macromolecules* **2002**, 35, 1632-1637.
438. Kaafarani, B. R.; Pinkerton, A. A.; **Neckers, D. C.** High order stacking of a perfluoro 'Y-enyne'. *Tetrahedron Lett.* **2001**, 42, 8137-8139.
439. Li, H.; Ren, K.; **Neckers, D. C.** Substituted cyclopropenium salts as photoinitiators for cationic polymerization of glycidyl phenyl ether. *Macromolecules* **2001**, 34, 8637-8640.
440. Wang, F.; Wu, X.; Pinkerton, A. A.; Kumaradhas, P.; **Neckers, D. C.** Photoreaction of platinum(II) β -diketonate complexes with olefins. *Inorg. Chem.* **2001**, 40 (23), 6000-6003.
441. Li, H.; Ren, K.; **Neckers, D. C.** Substituted cyclopropenium salts - photochemical, thermal reactions and mechanistic investigations. Presented at RadTech Conference, Basel, Switzerland, 2001.
443. Tyson, D. S.; Luman, C. R.; Zhou, X.; **Castellano, F. N.** New Ru(II) chromophores with extended excited-state lifetimes. *Inorg. Chem.* **2001**, 40, 4063-4071.
444. Wang, F.; **Neckers, D. C.** Photopolymerization of epoxides with platinum(II) bis(acetylacetonato)/silane catalysts. *Macromolecules* **2001**, 34, 6202-6205.
445. Ren, K.; Serguievski, P.; Gu, H.; Grinevich, O.; Malpert, J. H.; **Neckers, D. C.** Relative photoactivities of iodonium tetrakis(pentafluorophenyl)gallates measured by fluorescence probe techniques. *Macromolecules* **2002**, 35, 898-904.

446. Strehmel, V.; Stiller, B.; Strehmel, B.; Sarker, A. M.; **Neckers, D. C.** Photoinduced crosslinking of distyrylbenzene containing blockcopolymers for manufacture of new photoalignment layers. *Polym. Prepr.* **2001**, 42 (2), 749.
447. Tyson, D. S.; Henbest, K. B.; Bialecki, J.; **Castellano, F. N.** Excited state processes in ruthenium(II)/pyrenyl complexes displaying extended lifetimes. *J. Phys. Chem. A* **2001**, 105, 8154-8161.
448. Sarker, A. A.; Kaneko, Y.; **Neckers, D. C.** Synthesis of tetraorganylborate salts. Photogeneration of tertiary amines. *Chem. Mater.* **2001**, 13 (11), 3949-3953.
449. **Ullrich, B.**; Schroeder, R. Green emission and bandgap narrowing due to two-photon excitation in thin film CdS formed by spray pyrolysis. *Semicond. Sci. Technol.* **2001**, 16, L37.
450. Schroeder, R.; **Ullrich, B.**; Graupner, W.; Scherf, U. Excitation density and photoluminescence studies of polyfluorene excited by two-photon absorption. *J. Phys.: Condens. Matter* **2001**, 13, L313.
451. Navarro, J. A.; Myshkin, E.; De la Rosa, M. A.; **Bullerjahn, G. S.**; Hervas, M. The unique proline of the *Prochlorothrix hollandica* plastocyanin hydrophobic patch impairs electron transfer to photosystem I. *J. Biol. Chem.* **2001**, 276, 37501-37505.
453. Hervas, M.; Myshkin, E.; Navarro, J. A.; De la Rosa, M. A.; **Bullerjahn, G. S.** Proline 14 is impairing the electron transfer from plastocyanin to photosystem I in the prochlorophyte *Prochlorothrix hollandica*. In *Proceedings of the XIIth International Congress on Photosynthesis*; CSIRO Press: Sydney, 2001; pp S11-005.

For reprints of any of these publications, please write or e-mail the Center for Photochemical Sciences and refer to the reprint by number.

Advertising Special in *The Spectrum*

The Spectrum is distributed worldwide and on the WEB at no cost as a part of the outreach of the Center for Photochemical Sciences. In an effort to defray the increasing costs, we are now offering space for advertisements on a limited basis. Following are the prices for single issues and a special for four issues.*

Single Issue		Four Issue Special	
Full page – black and white	\$1200	Full page – black and white	\$4000
Full page – color	\$1800	Full page – color	\$6000
Half page – black and white	\$600	Half page – black and white	\$1800
Half page – color	\$900	Half page – color	\$3000
To reserve space e-mail pat.green@attbi.com		Deadline is June 15, 2002	

*The four issues can be any four of your choosing in 2002 and 2003.